Magazine of Concrete Research

Effect of calcium nitrate healing microcapsules on concrete strength and air permeability
Al-Ansari, Abu Taqa, Senouci, Hassan and Shaat

Magazine of Concrete Research
http://dx.doi.org/10.1680/jmacr.17.00435
Paper 1700435
Received 18/09/2017; revised 21/12/2017; accepted 22/12/2017
Keywords: compressive strength/cracks & cracking/modulus of elasticity

ice
Institution of Civil Engineers
publishing

Effect of calcium nitrate healing microcapsules on concrete strength and air permeability

Mohammed Al-Ansari
Associate professor, Department of Civil and Architectural Engineering, Qatar University, Doha, Qatar (Orcid:0000-0002-7467-8733)

Ala G. Abu Taqa
Postdoctoral associate, Department of Civil and Architectural Engineering, Qatar University, Doha, Qatar (corresponding author: ala.abutaqa@yahoo.com) (Orcid:0000-0002-6197-5296)

Ahmed Senouci
Associate professor, Department of Construction Management, University of Houston, Houston, TX, USA (Orcid:0000-0003-0735-9473)

Marwa M. Hassan
CETF distinguished associate professor, Department of Construction Managment, Louisina State University, Baton Rouge, LA, USA (Orcid:0000-0001-8087-8232)

Ahmed Shaat
Senior project manager, MZ & Partners Architectural & Engineering Consultancy, Doha, Qatar (Orcid:0000-0002-8668-476X)

This study investigates the compressive and flexural strengths, flexural modulus and air permeability of concrete samples containing 0·75% by cement weight of modified calcium nitrate self-healing microcapsules. The compressive and flexural strengths of concrete mixes with microcapsules were determined before healing and compared with those of the control mix. Moreover, another set of samples were loaded up to 60% of their ultimate load and placed in a water bath to accelerate their healing. The samples' air permeability was measured before loading, after applying 60% of the ultimate load, and after 3 and 7 d of healing. The stress–strain curves were plotted to determine the flexural modulus. The results show that there is a significant statistical difference in the compressive strengths of mixes with and without microcapsules. However, the mix flexural strength did not show a significant statistical effect. Scanning electron micrograph (SEM) images of the fracture surfaces of samples with microcapsules showed a good healing efficiency of calcium nitrate microcapsules. It was also found that the addition of microcapsules considerably decreased the samples' air permeability. Although the flexural moduli of samples containing microcapsules were found to be less than those of samples without microcapsules before healing, modulus recovery was reported after 7 d of self-healing.

Notation

A_s	area of tensile steel reinforcement
A'_s	area of compressive steel reinforcement
b	concrete section width
d	distance from the extreme compression fibre to the centroid of longitudinal tensile reinforcement
d'	distance from the extreme compression fibre to the centroid of the longitudinal compressive reinforcement
E_c	concrete modulus of elasticity
E_s	steel modulus of elasticity
f_c	concrete stress
f'_c	concrete average compressive strength
I_{cr}	cracked moment of inertia
kT	coefficient of air permeability
L	span length
M	applied load moment
P	applied load
P_u	ultimate load
s	sample standard deviation
x_i	test value
$\bar{x}$	average test value
ε_c	concrete strain
ε_c	average steel strain
η	modular ratio
κ	factor of depth of the neutral axis
μ	average value
ρ	tensile steel reinforcement ratio
ρ'	compressive steel reinforcement ratio

Introduction

Self-healing using microencapsulation (White *et al.*, 2001) is a promising alternative to the maintenance and repair of deteriorated concrete structures. On loading, the formation of cracks triggers the self-healing mechanism by rupturing the microcapsule shell and releasing the healing agent. The reaction between the released healing agents and the concrete catalysts forms products that fill the cracks and hinder their propagation.

Significant research work was reported in the literature on the encapsulation of various self-healing agents, such as sodium silicate and polyurethane (Kaes *et al.*, 2014; Pelletier *et al.*, 2015; Van-Tittelboom *et al.*, 2011). Dry (1994) reported the first microencapsulation attempts using methyl methacrylate within polypropylene and glass fibres. Other researchers (Li *et al.*, 1998; Mihashi *et al.*, 2000; Van-Tittelboom *et al.*, 2011) used brittle capillary tubes as encapsulation agents. Yang *et al.* (2011) encapsulated methyl methacrylate monomer in silica gel. Self-healing microcapsules were recently produced using urea formaldehyde (Wang *et al.*, 2013). Wang *et al.* (2013) reported a significant decrease in the flexural and compressive strengths of concrete specimens containing microcapsules in amounts larger than 3% by cement weight. Huang and Ye (2011) used sodium silicate solution as a self-healing agent in cementitious materials; sodium silicate forms calcium silicate hydrate (C–S–H) on contact with the calcium hydroxide (C–H) in the cement matrix. Mostavi *et al.* (2015) introduced in-situ polymerisation of sodium silicate in a double-walled polyurethane and urea-formaldehyde shell. However, the high cost of the aforementioned healing agents limited their application.

Hassan *et al.* (2016) made the first attempt to encapsulate calcium nitrate, as a low-cost self-healing agent of high reactivity with cement matrix, in a urea-formaldehyde shell. In fact, calcium nitrate includes cations that are found in dicalcium and tricalcium silicates (C2S, C3S). The nucleation of ions promotes the crystallisation of hydrates and hence accelerates the hydration process (Karagöl *et al.*, 2013; Ramachandran, 1995). Moreover, on the release of the healing agent in the crack, calcium ions (Ca^{2+}) in the calcium nitrate may participate in calcium carbonate deposition by increasing the calcite saturation index (Edvardsen, 1999). Accordingly, calcium nitrate may be a promising low-cost alternative to healing agents. It is worth noting that the reactions between calcium nitrate and cement matrix were not completely resolved and thus it is necessary to develop both kinetic and thermodynamic models to describe such reactions in order to understand the healing mechanism (Abdelrazig *et al.*, 1999; Balonis *et al.*, 2011; Justnes, 2003, 2010; Justnes and Nygaard, 1995; Ramachandran, 1995).

The encapsulation procedure of calcium nitrate developed by Hassan *et al.* (2016) used an in-situ polymerisation process to prepare the continuous phase using a water-in-oil emulsion and an oil-soluble sulfonic acid catalyst. The calcium nitrate microcapsules have shown a satisfactory healing efficiency, but they significantly reduced the strength of concrete mixes (Milla *et al.*, 2016). To reduce the adverse effect of calcium nitrate microcapsules on concrete strength, Al-Ansari *et al.* (2017) have proposed a modification to the calcium nitrate encapsulation procedure that was reported by Hassan *et al.* (2016). In their work, the authors have attributed the strength reduction in concrete mixes to the amount of sulfonic acid used for the preparation of the continuous phase in the procedure reported by Hassan *et al.* (2016), as sulfonic and other acids are hydration retarders (Singh *et al.*, 1986; Sobolkina *et al.*, 2012). Hence, the modified procedure altered the continuous-phase composition by reducing the amount of sulfonic acid catalyst and adding a low hydrophilic–lipophilic balance emulsifier. Al-Ansari *et al.* (2017) investigated the compressive and flexural strengths of mortar samples containing various concentrations of calcium nitrate microcapsules prepared using the modified encapsulation procedure. They have concluded that the proposed modification improved the mortar strength and resulted in a smaller reduction of the compressive and flexural strengths compared with those obtained using the original encapsulation method. The authors have also recommended a calcium nitrate microcapsule concentration of 0·75% (by weight of cement) to limit the reduction in the initial stiffness (elastic modulus) of the samples containing the microcapsules before healing.

This paper may be considered an extension to the previous study of the authors on mortar samples (Al-Ansari *et al.*, 2017). It describes an investigation of the effect of the calcium nitrate microcapsules prepared using the modified encapsulation procedure on the ultimate mechanical properties of reinforced and unreinforced concrete rather than mortar. It is very important to investigate the effect of the modified microcapsules on the mechanical properties of concrete, as previous studies reported a significant strength reduction, owing to the incorporation of calcium nitrate microcapsules prepared using the original encapsulation procedure (Hassan *et al.*, 2016; Milla *et al.*, 2016). The percentage of modified microcapsules that was recommended by Al-Ansari *et al.* (2017) for mortar (i.e. 0·75% by weight of cement) was incorporated into reinforced and unreinforced concrete samples and the associated reductions of the ultimate compressive and flexural strengths were investigated. Moreover, the effect of such microcapsules on the flexural (elastic) modulus and air permeability of concrete before and after healing was studied.

Experimental programme

Concrete mixes containing 0·75% of calcium nitrate microcapsules, by weight of cement, were first prepared using the modified encapsulation procedure. Then, the compressive and flexural strengths of these mixes were computed and compared with those of the control mix. Moreover, the initial flexural stiffness (modulus) before healing was determined for the control mixes and for those containing microcapsules. To study the effect of self-healing microcapsules on the air permeability, another set of concrete samples were loaded up to 60% of their ultimate (failure) load and their strains were measured. The Torrent method was used to measure the air permeability before loading and after applying 60% of the ultimate load (Torrent, 1992). After that, the samples were placed in a water bath to accelerate the healing process, and the air permeability was remeasured after 3 d and 7 d of healing. Finally, the samples were loaded up to failure and the stress–strain curves were plotted to examine the flexural modulus recovery due to healing. It is worth noting that applying such a level of loading (60% of the ultimate load) will induce wide cracks, where the effect of the intrinsic self-healing capability of concrete is limited. In accordance with Yildirim *et al.* (2015), the intrinsic crack closure in cementitious materials is attributed to the swelling of the existing hydrated products, continued hydration and calcium carbonate formation. Yildirim *et al*. (2015) have also reported that this effect may be restricted to tight micro-cracks with widths less than 100 μm. Accordingly, after applying 60% of the ultimate load on the samples and placing them in a water bath, the autogenous healing after unloading will be effective for micro-cracks only. Conversely, the effect of the self-healing due to the presence of microcapsules will be dominant for wide cracks.

Self-healing microcapsule preparation

The modified calcium nitrate encapsulation procedure proposed by Al-Ansari *et al*. (2017) was adopted for the microcapsule preparation. The procedure consists of dissolving the core materials, namely, urea, formaldehyde (37% solution), resorcinol, ammonium chloride and calcium nitrate, in distilled water to prepare the aqueous phase. The continuous-phase composition includes an organic solvent (hexane), a low hydrophilic–lipophilic balance emulsifier, and a small amount of a sulfonic acid soluble in oil. The continuous phase was then subjected to a high-shear agitation (1500 r/min) and heated to 40°C. The aqueous phase was then added dropwise to the continuous phase over a period of 10 min and the agitation was continued at the same speed and temperature for 1 h (Hassan *et al*., 2016; Milla *et al*., 2016). After the reaction had been completed, the produced microcapsules were allowed to settled at the bottom of the beaker for some time before the excess hexane was decanted and the microcapsule slurry was air dried. Figure 1 summarises the microcapsule synthesis. The amounts shown in the figure produce around 23–25 g of microcapsules.

Scanning electron microscopy

A Nova NanoSEM model scanning electron microscope was used to characterise the microcapsules and their healing efficiency. The microcapsules were scattered on top of a double-sided tape attached to a pin stub specimen mount. They were then sputter-coated with platinum for 4 min before imaging at an accelerating voltage of 20 kV.

To characterise the healing efficiency of the microcapsules, a sample of fracture surfaces of the hardened concrete that contains microcapsules was taken before healing and dried using vacuum. Then, the sample was coated using gold and palladium to dissipate excess charges and enhance image resolution. The sample was then placed in a water bath and allowed to heal for 7 d. Scanning electron micrographs were obtained after healing. A low-energy secondary electron imaging option was used to capture images.

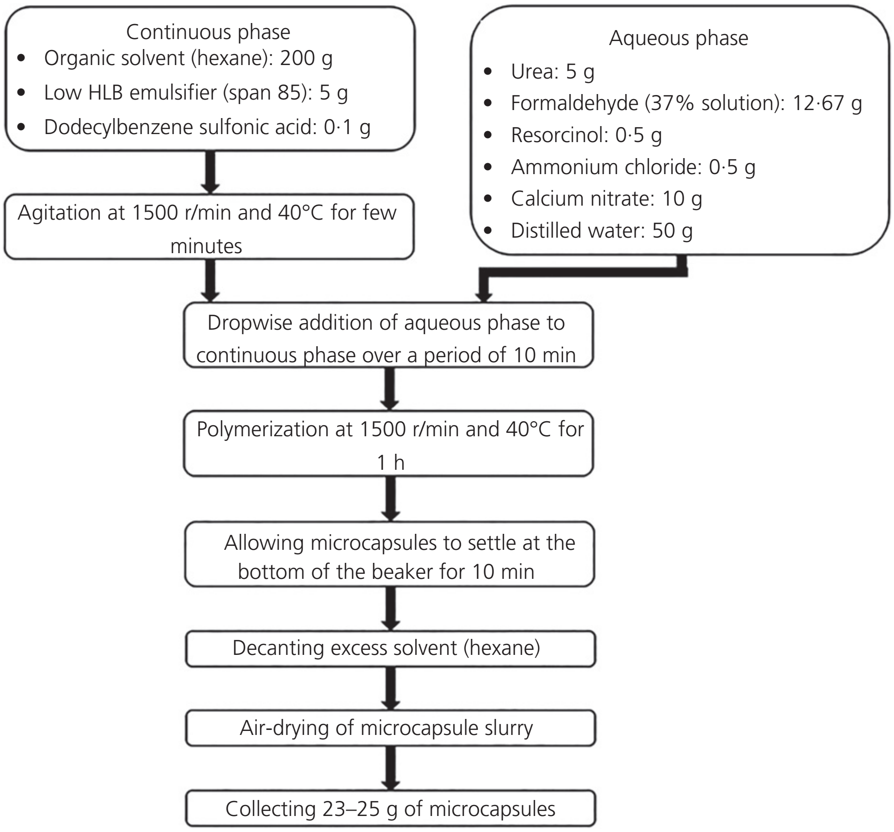

Figure 1. Modified synthesis of calcium nitrate microcapsules. HLB, hydrophilic–lipophilic balance

Concrete testing

Compressive and flexural strength tests were conducted on control concrete samples and those containing 0·75% calcium nitrate self-healing microcapsules (by weight of cement). All samples were casted and cured according to ASTM C 192 (ASTM, 2016a). The air permeability was also investigated on another set of samples before loading, after applying 60% of the ultimate load and after 3 and 7 d of accelerated healing. Moreover, the elastic modulus before and after healing was computed from the stress–strain curves. Material specifications, mixture composition and test setups are detailed next.

Mixture composition

All concrete mixes were prepared using Portland cement (CEM I) Class 42·5 R complying with EN 197-1, 10–20 mm and 4–10 mm diameter coarse aggregates, 0–4 mm diameter natural washed sand conforming to BS EN 12620 and tap water. The mix was provided by a ready-mix company for a 35 MPa concrete cubic strength with 0·45% free water/cement ratio. The self-healing concrete mixes contained 0·75% (by weight of cement) of calcium nitrate microcapsules. The mix compositions are summarised in Table 1.

Table 1. Mix designs

Constituent material	Control mix: kg/m^3	Self-healing mix: kg/m^3
Portland cement CEM I	500	500
Coarse aggregate 10–20 mm	578	578
Coarse aggregate 4–10 mm	272	272
Fine aggregate (natural washed sand)	762	762
Free water	225	225
Calcium nitrate microcapsules	Not applicable	3·75

Compressive and flexural strength tests

Nine standard cylinders (i.e. 152 mm in diameter and 304 mm in length) were prepared from each mix according to ASTM C 470 (ASTM, 2015) and tested in compression after 28 d of moist curing according to ASTM C 39 (ASTM, 2016b).

The flexural strength test was performed on plain and steel-reinforced beams with a cross-section of 150 mm × 150 mm and a length of 750 mm. Six beams were cast from each mix. Three beams were plain concrete and three were reinforced with 2T10 on the bottom and 2T8 on the top of Grade 60 reinforcing steel bars satisfying ASTM A 615M (ASTM, 2016c). Six T8 Grade 60 steel stirrups were provided in each beam, as shown in Figure 2. A three point bending flexural test was conducted to determine the flexural load.

Air permeability and flexural modulus tests

A Torrent permeability tester (Torrent, 1992) was used to investigate the effect of self-healing microcapsules on the air permeability of samples and measure the air permeability coefficients (kT) at their cracked surfaces (Figure 3). This method involves using a vacuum pump to create an air depression in a two-chamber cell placed on the concrete surface. The essential features of the Torrent tester are a two-chamber cell (test chamber and surrounding guard ring) and a regulator to manage the pressure in the guard ring (outer) chamber and keep it always equal to that of the test (inner) chamber. This will achieve a unidirectional air flow into the inner chamber and eliminate any pseudolateral air flow. The pressure rise in the chamber, induced by the flow of air through the concrete, is measured as a function of time and the rate at which the pressure returns to the atmospheric value is recorded. The coefficient of air permeability is calculated as a function of the pressure variation with time and other characteristic values. Figure 4 illustrates the principle of the Torrent method for testing air permeability.

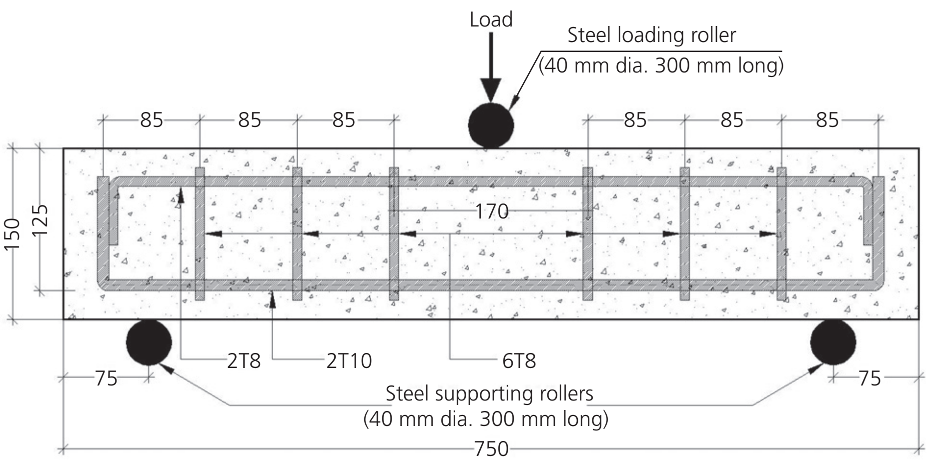

Figure 2. Beam steel reinforcement details; dimensions in mm

Another set of six 150 × 150 × 750 mm beams were prepared from each mix (i.e. three plain concrete beams and three steel-reinforced beams, as shown in Figure 1). Type FLA-5-11 strain gauges with a length of 5 mm, supplied by Tokyo Sokki Kenkyujo, were fixed to each of the bottom reinforcing bars, as shown in Figure 5. These strain gauges measure the flexural strains needed to calculate the flexural modulus.

To install each strain gauge at the midpoint of the bottom (tension) bars, a flat surface area was created to fit the strain gauge. This area was then abraded with silicon-carbide paper grits 320 and 400 and cleaned with acetone. The strain gauge was attached to the created flat area using a cyanoacrylate adhesive. A butyl rubber (SB tape) was applied under the gauge lead wire prior to the over-coating, as shown in the left part of Figure 6. Then, two layers of protective coating were applied to the gauge as a first coating. Finally, the strain gauge was wrapped with a butyl rubber tape (VM tape) and covered with silicone rubber to protect it from any damage during concrete pouring, as shown in the right part of Figure 6.

The beam samples were tested for air permeability in two locations before loading, as shown in Figure 7. They were then loaded to 60% of their ultimate loads. The strain gauges were attached to a data logger to record the loads and strains every second. The air permeability was measured after loading at the same locations tested before loading. The samples were then placed in a water bath to accelerate the healing process. The air permeability was remeasured after 3 and 7 d of healing. Finally, the samples were removed from the water bath and loaded up to failure, while the strain gauges were reattached to the data logger to measure strains after healing.

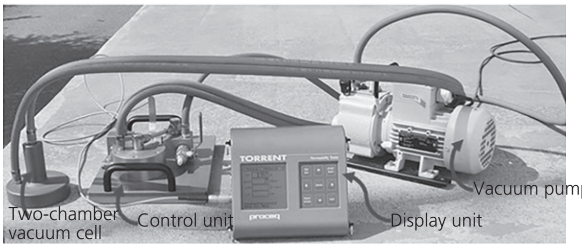

Figure 3. Torrent air permeability tester

Results and analysis

Scanning electron microscopy

Figure 8 presents the scanning electron micrographs that were used to characterise the prepared microcapsules. The average diameter of the prepared microcapsules was around 60 μm, while the average shell thickness was around 1 μm. This is in good agreement with the findings of Hassan *et al*. (2016), who obtained a microcapsule average diameter of 51 μm and a shell thickness of 0·91 μm using the same preparation parameters. Hassan *et al*. (2016) have also reported an optimum healing efficiency by incorporating microcapsules with an average diameter of 58·7 μm.

Figure 9 shows scanning electron micrographs of a sample containing 0·75% microcapsules by weight of cement before healing and after 7 d of healing, respectively. The micrographs show that the microcapsules had a good efficiency in healing the cracks.

Compressive and flexural strengths

Tables 2 and 3 summarise the compressive and flexural strengths results of all mixes after 28 d of moist curing. The results are reported to two decimal places, which is justified by the test precision. It is worth noting that the presence of

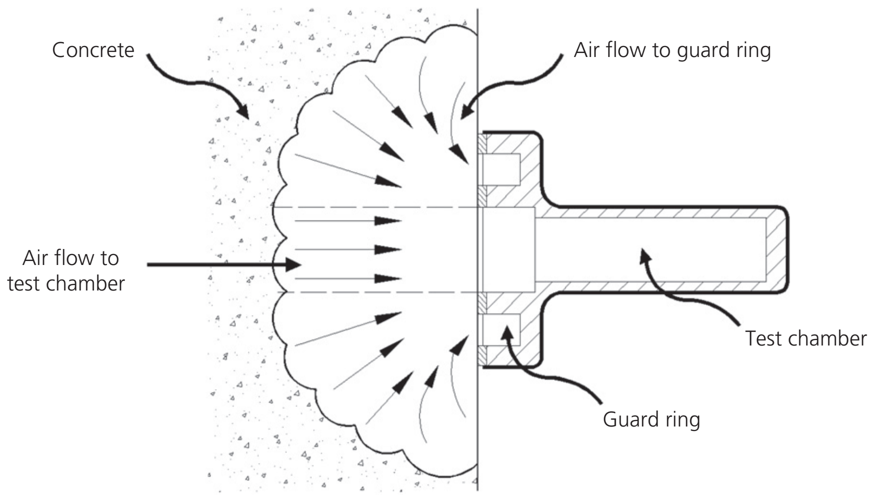

Figure 4. Torrent air permeability test principle

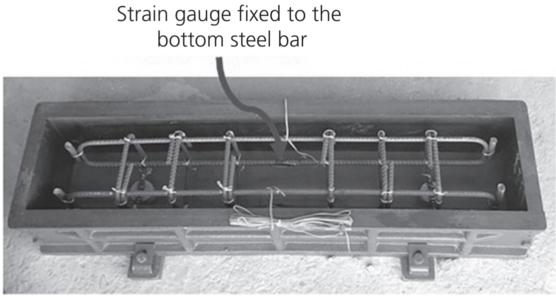

Figure 5. Strain gauges fixed to bottom steel bars of reinforced concrete beams

Figure 6. Strain gauge installation to steel bar

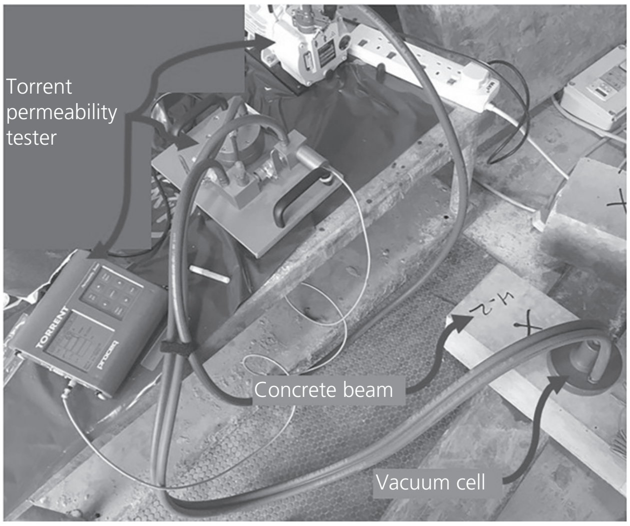

Figure 7. Concrete beam air permeability testing

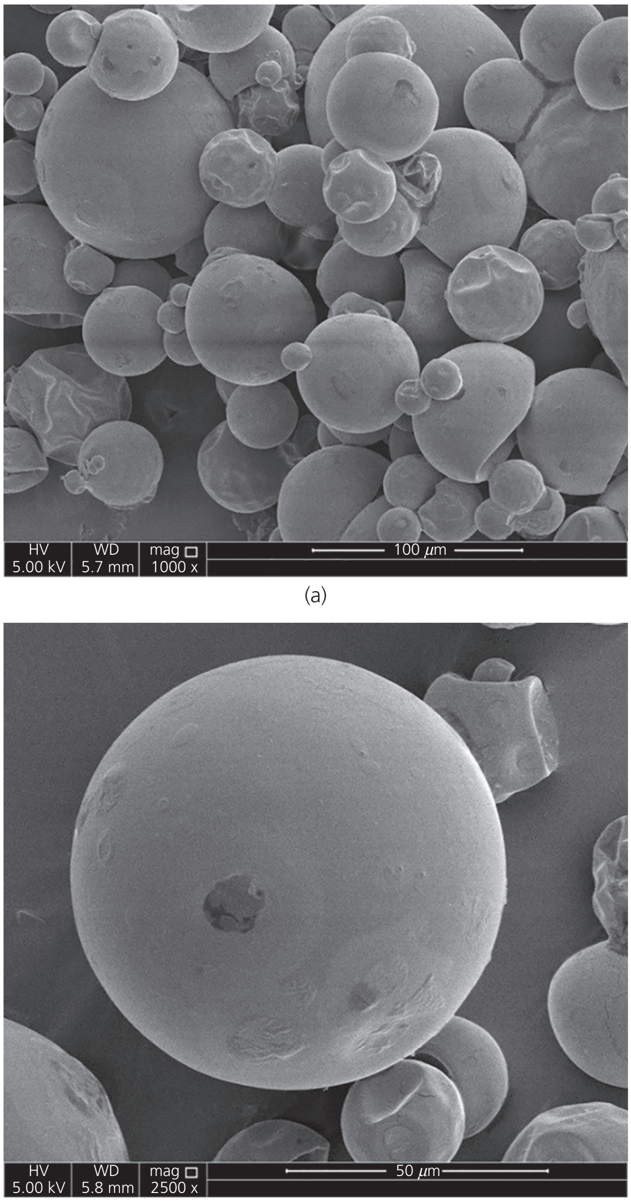

Figure 8. Scanning electron micrographs of prepared microcapsules: (a) group of microcapsules; (b) single microcapsule

outlying observations should be first determined for all tests to identify samples that deviate significantly from the rest. This is an important check during the analysis of the test results because the underlying observations may result from several sources, such as recording error, numerical calculation error or equipment error. Outlying observations, which were identified according to ASTM E 178 (ASTM, 2008) before computing the average of the test readings, were excluded from the data. The ASTM E 178 standard states that an observation is considered an outlier for a 5% one-sided significance level if the absolute values of the test statistic shown in Equation 1 exceed the critical values of 1·822 and 1·153 for six and three repetitions, respectively.

1. $$\varepsilon_i = (x_i - \bar{x})/s$$

where ε_i is the test statistic value, x_i the test value, $\bar{x}$ the average test value and the sample standard deviation.

Tables 2 and 3 show that the compressive and flexural strengths decreased for the mix containing self-healing microcapsules. The reduction in the 28 day compressive strength was

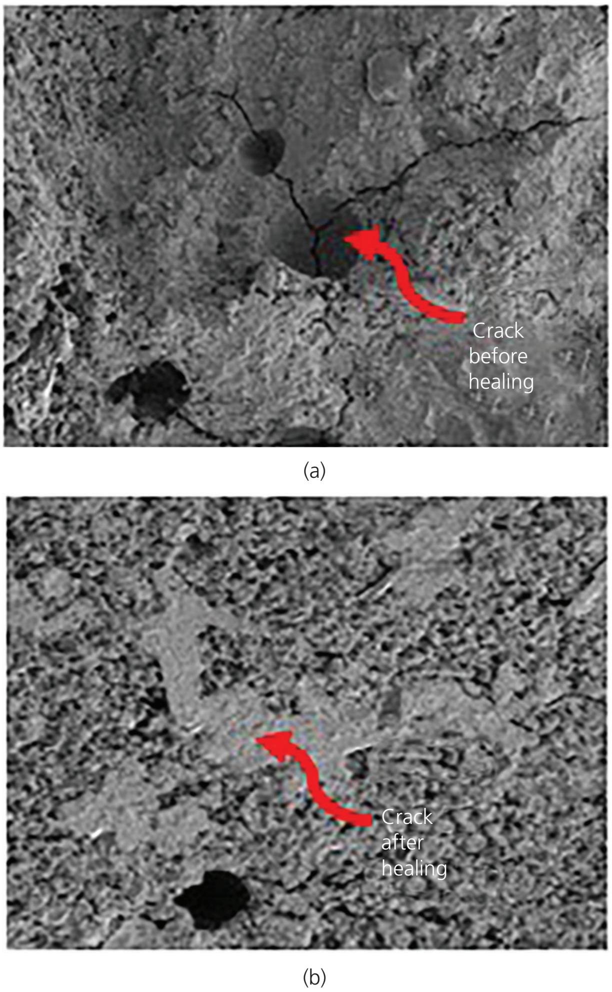

Figure 9. Crack scanning electron micrographs: (a) before healing; (b) after 7 d of healing

Table 2. 28 d compressive strength results: MPa

Sample no.	Control mix	Self-healing mix
1	36·69	30·93
2	30·80	30·41
3	36·79	31·07
4	32·58	30·45
5	31·03	29·14
6	22·67 (outlier)	29·89
7	34·72	30·90
8	36·17	29·11
9	33·68	29·78
Average: μ	**34·06**	**30·19**
Standard deviation: s	**2·6**	**0·75**

approximately 11%, which is less than the 33% and 73% reductions reported by Milla *et al*. (2016) for concrete beams containing 1·20% and 2·00% microcapsules by weight of cement, respectively. Conversely, the flexural strength reductions were found to be approximately 14% and 2% for plain

Table 3. 28 d flexural strength results: MPa

	Sample no.	Control mix	Self-healing mix
Plain concrete	1	4·16	4·24
	2	4·99	4·05
	3	5·52	4·27
	Average: μ	**4·89**	**4·19**
	Standard deviation: s	**0·69**	**0·12**
Steel-reinforced concrete	1	41·17	40·77
	2	40·38	41·49
	3	42·67	39·85
	Average: μ	**41·41**	**40·71**
	Standard deviation: s	**1·17**	**0·82**

and steel-reinforced concrete samples, respectively. It can be concluded that using 0·75% calcium nitrate microcapsules by cement weight prepared using the modified encapsulation procedure can lower the strength reduction associated with incorporating calcium nitrate self-healing microcapsules into concrete, compared with the original encapsulation procedure.

Statistical Student's t tests were used to determine whether there are statistical differences between the strengths of the control mix and that containing microcapsules. The null hypothesis assumed that the average strength values of both mixes were equal (i.e. $\mu_{\text{control mix}} = \mu_{\text{self-healing mix}}$). Considering a two-tailed significance level of 0·05 ($\alpha = 0{\cdot}05$), Table 4 shows the t statistics and critical t test values for the compressive and flexural strengths. The null hypothesis is rejected if the t statistic is larger than or equal to the critical t test value. It is worth noting that some texts suggest that the degree of freedom is approximated by the smaller of $n_1 - 1$ and $n_2 - 1$ (where n_1 and n_2 are the sizes of sample 1 and sample 2, respectively). However, the following equation shall be used in a t statistical test to compare the means of two independent samples

$$2. \quad \text{Degree of freedom} = \frac{\left[(s_1^2/n_1) + (s_2^2/n_2)\right]^2}{\left[\left[(s_1^2/n_1)^2/(n_1-1)\right] + \left[(s_2^2/n_2)^2/(n_2-1)\right]\right]}$$

where n_1 is the size of sample 1, n_2 is the size of sample 2, s_1 is the standard deviation of sample 1 and s_2 is the standard deviation of sample 2.

It should be noted that in Equation 2 the degree of freedom is a function of the sample size and its standard deviations. This justifies the different degrees of freedom of the plain and reinforced samples used for the statistical t test with the same sample size but different standard deviations, as shown in Table 4.

Table 4 shows that the null hypothesis is rejected for the compressive strength and accepted for the flexural strengths

Table 4. Compressive and flexural strength result *t* test analysis

		Degree of freedom	Standard error	*t* statistic value	Critical *t* test value
Compressive strength		8	0·896	4·32	2·306
Flexural strength	Plain concrete	2	0·402	1·75	4·303
	Reinforced concrete	4	0·823	0·86	2·776

Table 5. Air permeability coefficient, kT ($\times 10^{-16}$ m^2)

		Control mix				Self-healing mix			
	Sample no.	Before loading	After applying 60% P_u	After 3 d of healing	After 7 d of healing	Before loading	After applying 60% P_u	After 3 d of healing	After 7 d of healing
Plain concrete	1	0·357 (16·5)[a]	0·395 (16·8)	0·360 (16·3)	0·324 (10·7)	1·655 (39·6)	1·813 (56·9)	0·930 (30·4)	0·031 (11·2)
	2	0·379 (42·6)	0·514 (45·4)	0·499 (44·6)	0·430 (39·9)	0·911 (41·4)	1·582 (56·3)	0·822 (32·6)	0·046 (15·4)
	3	0·218 (32·1)	0·570 (46·6)	0·459 (44·2)	0·432 (42·9)	0·840 (41·2)	0·979 (50·5)	0·624 (29·2)	0·028 (12·1)
Steel-reinforced concrete	1	0·397 (39·5)	0·448 (48·2)	0·429 (46·7)	0·410 (45·3)	0·612 (38·2)	0·941 (49·5)	0·591 (24·3)	0·018 (14·3)
	2	0·395 (25·2)	0·535 (34·4)	0·528 (33·3)	0·487 (31·6)	0·619 (37·8)	0·934 (47·3)	0·418 (21·1)	0·015 (11·3)
	3	0·295 (19·8)	0·398 (30·2)	0·374 (28·6)	0·362 (28·4)	0·622 (40·1)	0·916 (45·2)	0·632 (23·9)	0·014 (13·4)

[a]Vacuum penetration depth (crack depth): mm

of plain and reinforced concrete. This implies that incorporating self-healing microcapsules in concrete has a significant statistical effect on the mix compressive strength. Conversely, it has an insignificant statistical effect on the mix flexural strength.

Air permeability test

The air permeability coefficient (kT) and the vacuum penetration depth were measured at two locations on the bottom surface of each tested beam, on both sides of the midpoint where the load was applied and cracks were likely to form. The average value of the two measured permeability values was recorded. These tests were repeated at the same locations on the cracked surface after loading the samples up to 60% of their ultimate loads. All samples, including those of the control mix, were placed in water to accelerate the healing process. The air permeability test was performed again after 3 and 7 d of placing the samples in water. Table 5 summarises the average values of the air permeability coefficients and the vacuum penetration depths for all samples.

For normal quality concrete, the air permeability coefficient lies in the range $0{\cdot}1 \times 10^{-16}$ to $1{\cdot}0 \times 10^{-16}$ m^2. However, the concrete may be defined as having a 'good' or 'very good' quality if the air permeability coefficient is less than $0{\cdot}1 \times 10^{-16}$ m^2. Table 5 shows that all air permeability coefficient values of both mixes lie within the range of normal quality concrete except those recorded for samples containing self-healing microcapsules after 7 d of healing, which were found to be less than $0{\cdot}1 \times 10^{-16}$ m^2. This is an indication that incorporating self-healing microcapsules improved concrete mix quality after 7 d of accelerated healing.

The reduction in the concrete air permeability over time may be attributed to many reasons. The CCAA datasheets (CCAA, 2006) report that extending the period of curing reduces the permeability of cement paste over time because water curing causes hydration products to fill existing pores and capillaries, either partially or completely. Moreover, a study of Huang *et al*. (2016) provided new insights into autogenous self-healing, where the decrease in capillary porosity of the matrix adjacent to the crack surfaces was quantified using nuclear magnetic resonance. Huang *et al*. (2016) attributed the reduction in the water content adjacent to the crack surface to the additional hydration of unhydrated cement particles in the bulk paste during the process of autogenous self-healing caused by the water coming from the crack. Conversely, the degradation of concrete permeability may also be caused by the self-healing microcapsules. It is worth noting that all samples of both mixes in this study were placed in water under the same conditions so that the effects of the extended curing and autogenous healing could be excluded and meaningful conclusions could be drawn about the self-healing effect of microcapsules on concrete permeability.

Figures 10 and 11 show the variation of the air permeability coefficients at all test stages for plain and steel-reinforced concrete samples, respectively. Figures 10 and 11 and Table 5 show that the air permeability coefficient and depth of vacuum penetration of both mixes increased after being subjected to 60% of the ultimate load. Moreover, the air permeability coefficient and vacuum penetration depth are larger for the self-healing mix, before the healing. This is an indication that the microcapsules increase the permeability of the concrete mix before the healing effect takes place. However, these values started to decrease after placing the samples in water (accelerating the

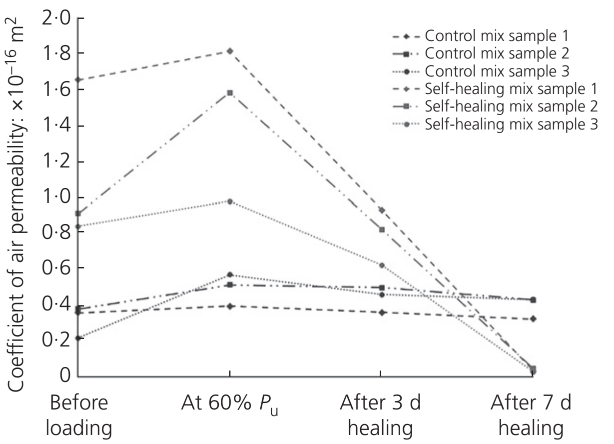

Figure 10. Plain concrete air permeability coefficient variation

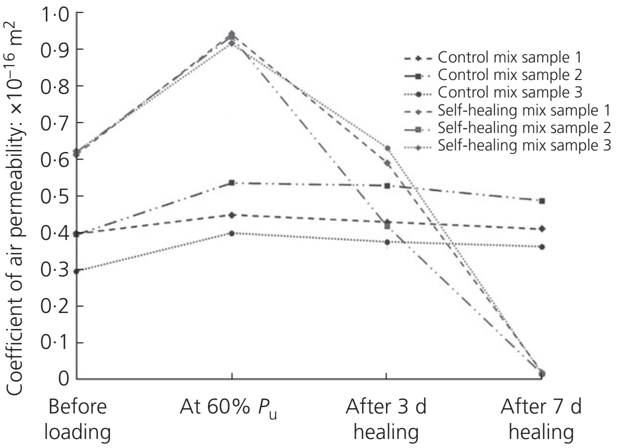

Figure 11. Steel-reinforced concrete air permeability variation

healing process). Figures 10 and 11 also show that the degradation rate in the control mix is less than that in the mix containing self-healing microcapsules. The reduction of the permeability of the control mix may be justified by the fact that the extended curing time reduces the permeability of concrete (CCAA, 2006) and also the autogenous self-healing process (Huang *et al.*, 2016). Conversely, the reduction of the permeability of the mix containing microcapsules can be attributed to the aforementioned effects and also to the effect of the self-healing microcapsules. After 7 d of healing, the concrete mix containing self-healing microcapsules becomes less permeable than the control mix because of the additional healing caused by the microcapsules.

Flexural modulus

The elastic modulus was calculated using the strain at the bottom flexural reinforcing bars during the flexural loading, as explained in Section 'Air permeability and flexural modulus tests'. To calculate the concrete strain, the depth of the neutral axis (κd) was first calculated as

3. $$\kappa d = \left[\left[(\rho+\rho')^2\eta^2 + 2\left(\rho + \frac{\rho' d'}{d}\right)\eta\right]^{1/2} - (\rho+\rho')\eta\right] d$$

where d is the distance from the extreme compression fibre to the centroid of longitudinal tensile reinforcement (in mm), d' is the distance from the extreme compression fibre to the centroid of longitudinal compressive reinforcement (in mm), ρ is the tension steel reinforcement ratio and ρ' is the compression steel reinforcement ratio.

The modular ratio η is computed using

4. $$\eta = E_s/E_c$$

where E_s is the steel modulus of elasticity.

The initial estimate of the concrete modulus of elasticity (E_c) is computed using the following equation (ACI 318, Equation 19.2.2.1.b) (ACI, 2014)

5. $$E_c = 4700\sqrt{f'_c}: \quad \text{MPa}$$

where f'_c is the average compressive strength of concrete in MPa.

The concrete strain in concrete is calculated as

6. $$\varepsilon_c = \varepsilon_s\, d/(d - \kappa d)$$

where ε_c is the concrete strain and ε_s is the average steel strain.

To calculate the flexural (elastic) modulus, the stress in concrete associated with each strain value should be calculated as well. The stress in concrete (in MPa) is computed as

7. $$f_c = M \times \kappa d/I_{cr}$$

where M is the moment corresponding to the applied load, in N.mm, and

8. $$M = PL/4$$

where P is the applied load, in N, L is the span length, in mm and I_{cr} is the cracked moment of inertia (in mm^4) of the section, calculated as

9. $$I_{cr} = \frac{1}{3}b(\kappa d)^3 + \eta A_s(d-\kappa d)^2 + \eta A'_s(\kappa d - d')^2$$

where b is the width of the concrete section (in mm), A_s is the area of tensile steel reinforcement (in mm^2) and A'_s is the area of the compressive steel reinforcement (in mm^2).

Table 6. Steel-reinforced concrete flexural modulus before and after healing for 7 d

	Control mix: GPa		Self-healing mix: GPa	
Sample no.	Before healing	After healing	Before healing	After healing
1	29·85	30·83	27·80	31·70
2	32·16	32·59	26·26	30·46
3	31·46	31·89	28·72	31·10
Average: μ	**31·16**	**31·77**	**27·59**	**31·09**
Standard deviation: s	**1·18**	**0·89**	**1·24**	**0·62**

Table 7. Steel-reinforced concrete flexural breaking loads before and after healing for 7 d

	Control mix: kN		Self-healing mix: kN	
Sample no.	Before healing	After healing	Before healing	After healing
1	88·92	89·86	86·34	90·67
2	88·28	87·86	87·11	90·45
3	91·14	90·86	87·33	89·93
Average: μ	**89·45**	**89·53**	**86·93**	**90·35**
Standard deviation: s	**1·50**	**1·53**	**0·52**	**0·38**

Finally, the flexural (elastic) modulus of concrete was calculated as the slope of the stress–strain curve from zero stress to the point where the stress in concrete (calculated in Equation 7) reaches $0{\cdot}45f'_c$, following ACI 318.19.2.2 (ACI, 2014). Table 6 shows the values of the flexural modulus calculated directly after applying 60% of the ultimate load (before healing) and after 7 d of healing for both mixes (reported to two decimal places, as justified by the test precision).

Moreover, Table 7 compares the flexural breaking load values of unhealed samples to those of the samples that were subjected to 7 d healing for both mixes.

Tables 6 and 7 show that, before healing, the average flexural modulus and flexural breaking load of the samples containing microcapsules were less than those of samples without microcapsules. They also show that the flexural modulus and the flexural breaking loads of the control mix samples were almost the same before healing and after being placed in the water bath for 7 d. However, the full recovery of the flexural modulus and flexural strengths occurred in the samples containing microcapsules, as a result of the healing effect, after 7 d.

The healing efficiency of the microcapsules justifies the aforementioned findings. On loading and cracking, the microcapsule shells were ruptured and released the healing agent. However, as the healing effect just started at that point, the locations in the samples that were filled with microcapsules might be considered as 'additional voids' and hence decreases in the flexural stiffness and load were observed. After 7 d of accelerated healing, these locations and the initiated cracks were filled with the healing agent, which increased the sample stiffness and strength. The scanning electron micrograph of one sample containing microcapsules after 7 d healing shown in Figure 12 supports this justification. It can be noted from the figure that the healing agent filled the microcapsule location and the adjacent crack, resulting in stiffness and strength recovery.

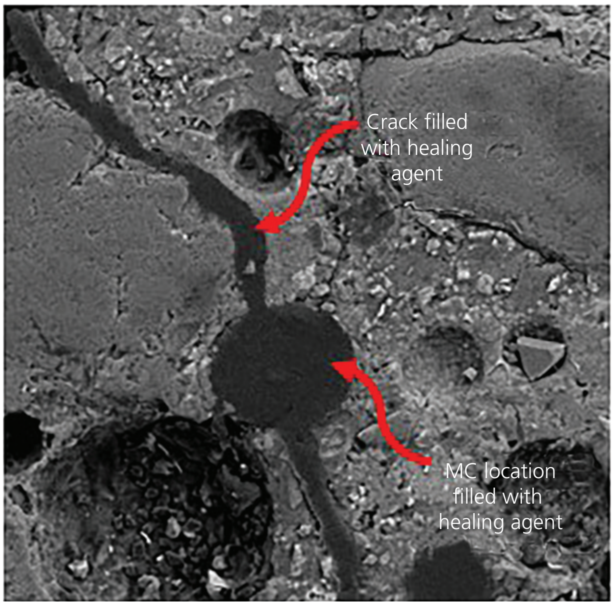

Figure 12. Scanning electron micrograph of healed area. MC, microcapsule

The scanning electron micrographs captured at arbitrary locations of different samples showed different cracking patterns in the control mix and self-healing mix after 7 d of healing. Figure 13 shows scanning electron micrographs at the same scale of a control mix sample and a self-healing mix sample after 7 d of healing, respectively. The micrographs show that the control mix sample contains significantly more cracks than the self-healing mix sample. Moreover, Figure 13(b) shows different healed areas in the sample containing microcapsules around the ruptured microcapsule locations (black circles). Conversely, Figure 13(a) does not show the same pattern in the control mix sample. These observations demonstrate the enhancement of the self-healing mix properties that occurred after healing, owing to the presence of microcapsules. They also prove the microcapsules' self-healing capabilities.

Conclusions

The mechanical properties (compressive and flexural strengths and flexural modulus) and the air permeability of unreinforced and reinforced concrete samples containing 0·75% by weight of

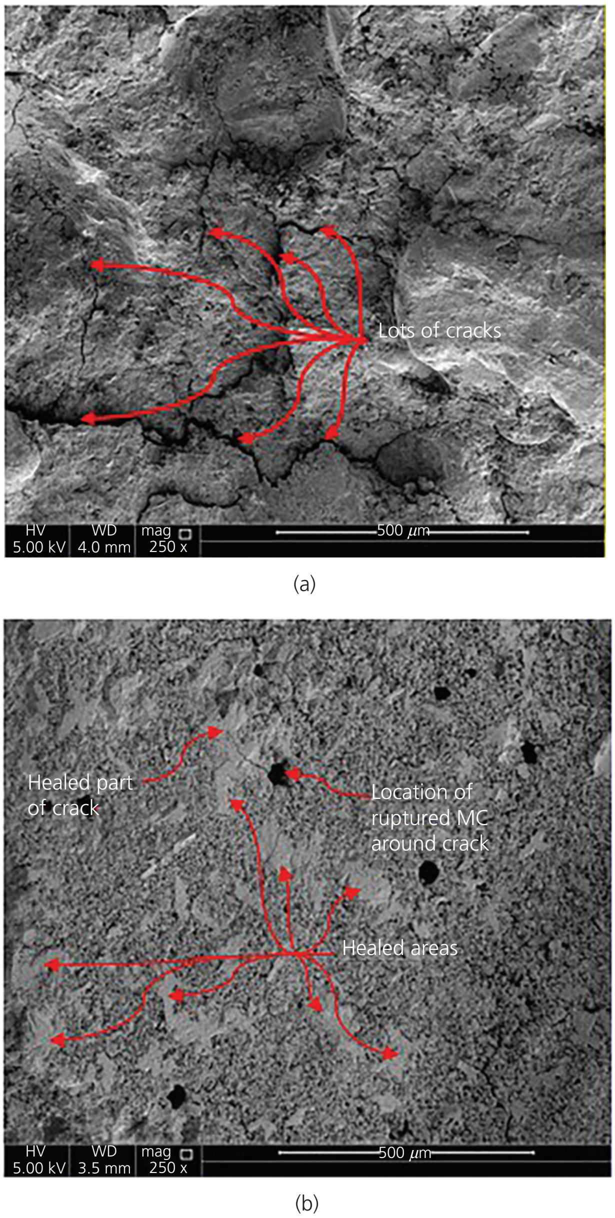

Figure 13. Scanning electron micrograph after 7 d of healing: (a) control sample; (b) self-healing sample. MC, microcapsule

cement of modified calcium nitrate self-healing microcapsules were investigated in this study. These properties were determined before healing, after applying 60% of the ultimate load, and after 3 and 7 d of accelerated healing. They were also compared with those of a control mix. Based on the results of the experimental study, the following conclusions can be drawn.

- The proposed encapsulation method yielded a lower reduction of both compressive and flexural strengths than the original encapsulation method.
- The reduction in the 28 day compressive strength was approximately 11% while the reductions in the flexural strength of plain and steel-reinforced samples were 14% and 2% respectively. *t* test analysis showed a statistically significant reduction in the compressive strength, while the reduction in the flexural strength was found to be statistically insignificant.
- Scanning electron micrographs of a sample taken before healing and after 7 d of healing showed that the microcapsules had a good healing efficiency.
- After cracking and before healing, the air permeability coefficient and the vacuum penetration depth of the samples containing self-healing microcapsules were higher than those of the control mix. However, it was found that, over time, the concrete permeability was reduced, owing to the microcapsules' healing effect, in addition to the effects of the extended curing and autogenous healing. This results in a less permeable concrete after 7 d of accelerated healing for the samples containing self-healing microcapsules. Hence, it may be concluded that incorporating self-healing microcapsules in concrete mixes reduces the permeability and promotes quality and durability.
- The flexural modulus and breaking loads of the samples containing 0·75% microcapsules by cement weight were found to be less than those of the control mix before healing. However, the full recovery of the flexural modulus and strength was recorded after 7 d of accelerated healing.

Acknowledgement

This work was made possible by a National Priority Research Program award (NPRP 6-280-2-117) from the Qatar National Research Fund (a member of The Qatar Foundation). The statements made herein are solely the responsibility of the authors.

REFERENCES

Abdelrazig BEI, Bonner DG, Nowell DV, Dransfield JM and Egan PJ (1999) The solution chemistry and early hydration of ordinary Portland cement pastes with and without admixtures. *Thermochimica Acta* **340–341**: 417–430.

ACI (American Concrete Institute) (2014) ACI 318M-14: Building code requirements for structural concrete and commentary. American Concrete Institute, Farmington Hills, MI, USA.

Al-Ansari M, Abu-Taqa A, Hassan M, Senouci A and Milla J (2017) Performance of modified self-healing concrete with calcium nitrate microencapsulation. *Construction and Building Materials* **149**: 525–534.

ASTM (2008) E 178: Standard practice for dealing with outlying observations. ASTM International, West Conshohocken, PA, USA.

ASTM (2015) C 470/C 470M: Standard specification for molds for forming concrete test cylinders vertically. ASTM International, West Conshohocken, PA, USA.

ASTM (2016a) C 192/C 192M: Standard practice for making and curing concrete test specimens in the laboratory. ASTM International, West Conshohocken, PA, USA.

ASTM (2016b) C 39/C 39M: Standard test method for compressive strength of cylindrical concrete specimens. ASTM International, West Conshohocken, PA, USA.

ASTM (2016c) A 615/A 615M: Standard specification for deformed and plain carbon-steel bars for concrete reinforcement. ASTM International, West Conshohocken, PA, USA.

Balonis M, Mędala M and Glasser FP (2011) Influence of calcium nitrate and nitrite on the constitution of AFm and AFt cement hydrates. *Advances in Cement Research* **23(3)**: 129–143.

CCAA (Cement Concrete and Aggregates Australia) (2006) *Datasheets: Curing of Concrete*. Cement Concrete & Aggregates Australia, Mascot, NSW, Australia.

Dry C (1994) Matrix cracking repair and filling using active and passive modes for smart timed release of chemicals from fibers into cement matrices. *Smart Materials and Structures* **3(2)**: 118–123.

Edvardsen C (1999) Water permeability and autogenous healing of cracks in concrete. *ACI Materials Journal* **96(4)**: 448–454.

Hassan M, Milla J, Rupnow T, Al-Ansari M and Daly B (2016) Micro-encapsulation of calcium nitrate for concrete applications. *Transportation Research Record* **2577**: 8–16.

Huang H and Ye G (2011) Application of sodium silicate solution as self-healing agent in cementitious materials. In *Proceedings of International RILEM Conference on Advances in Construction Materials through Science and Engineering, Hong Kong* (Leung C and Wan KT (eds)). RILEM Publications, Hong Kong, China, pp. 530–536.

Huang H, Ye G and Pel L (2016) New insights into autogenous self-healing in cement paste based on nuclear magnetic resonance (NMR) tests. *Materials and Structures* **49(7)**: 2509–2524.

Justnes H (2003) Explanation of long-term compressive strength of concrete cause by the set accelerator calcium nitrate. In *Proceedings of 11th International Congress on the Chemistry of Cement (ICCC): Cement's Contribution to the Development in the 21st Century, Durban, South Africa* (Grieve G and Owens G (eds)). Cement and Concrete Institute of South America, Durban, South Africa, pp. 475–484.

Justnes H (2010) Calcium nitrate as multifunctional concrete admixture. *International Analytical Review 'Alitinform'* **16(4–5)**: 38–45.

Justnes H and Nygaard EC (1995) Technical calcium nitrate as set accelerator for cement at low temperatures. *Cement and Concrete Research* **25(8)**: 1766–1774.

Kaes M, Van-Tittelboom K and De-Belie N (2014) The efficiency of self-healing cementitious materials by means of encapsulated polyurethane in chloride containing environments. *Construction and Building Materials* **71**: 528–537.

Karagöl F, Demirboğa R, Kaygusuz MA, Yadollahi MM and Polat R (2013) The influence of calcium nitrate as antifreeze admixture on the compressive strength of concrete exposed to low temperatures. *Cold Regions Science and Technology* **89**: 30–35.

Li VC, Lim YM and Chan YW (1998) Feasibility study of a passive smart self-healing cementitious composite. *Composites Part B: Engineering* **29(6)**: 819–827.

Mihashi H, Kaneko Y, Nishiwaki T and Otsuka K (2000) Fundamental study on development of intelligent concrete characterized by self-healing capability for strength. *Transactions of the Japan Concrete Institute* **22(2)**: 441–450.

Milla J, Hassan M, Rupnow T, Al-Ansari M and Arce G (2016) Effect of self-healing calcium nitrate microcapsules on concrete properties. *Transportation Research Record* **2577**: 69–77.

Mostavi E, Asadi S, Hassan M and Alansari M (2015) Evaluation of self-healing mechanisms in concrete with double-walled sodium silicate microcapsules. *Journal of Materials in Civil Engineering* **27(12)**: 04015035.

Pelletier M, Brown R, Shukla A and Bose A (2015) *Self-healing Concrete with a Microencapsulated Healing Agent*. See http://citeseerx.ist.psu.edu/viewdoc/download?doi=10.1.1.653.7244&rep=rep1&type=pdf (accessed 28/01/2018).

Ramachandran VS (1995) *Concrete Admixtures Handbook*, 2nd edn. Noyes Publications, Saddle River, NJ, USA.

Singh NB, Singh AK and Prabha-Singh S (1986) Effect of citric acid on the hydration of Portland cement. *Cement and Concrete Research* **16(6)**: 911–920.

Sobolkina A, Mechtcherine V, Khavrus V *et al.* (2012) Dispersion of carbon nanotubes and its influence on the mechanical properties of the cement matrix. *Cement & Concrete Composites* **34(10)**: 1104–1113.

Torrent RJ (1992) A two-chamber vacuum cell for measuring the coefficient of permeability to air of the concrete cover on site. *Materials and Structures* **25(6)**: 358–365.

Van-Tittelboom K, De-Belie N, Van-Loo D and Jacobs P (2011) Self-healing efficiency of cementitious materials containing tubular capsules filled with healing agent. *Cement and Concrete Composites* **33(4)**: 497–505.

Wang X, Xing F, Zhang M, Han N and Qian Z (2013) Experimental study on cementitious composites embedded with organic microcapsules. *Materials* **6(9)**: 4064–4081.

White SR, Sottos NR, Geubelle PH *et al.* (2001) Autonomic healing of polymer composites. *Nature* **409(6822)**: 794–797.

Yang Z, Hollar J, He X and Shi X (2011) A self-healing cementitious composite using oil core/silica gel shell microcapsules. *Cement and Concrete Composites* **33(4)**: 506–512.

Yildirim G, Keskin ÖK, Keskin SB, Sahmaran M and Lachemi M (2015) A review of intrinsic self-healing capability of engineered cementitious composites: recovery of transport and mechanical properties. *Construction and Building Materials* **101**: 10–21.

How can you contribute?

To discuss this paper, please submit up to 500 words to the editor at journals@ice.org.uk. Your contribution will be forwarded to the author(s) for a reply and, if considered appropriate by the editorial board, it will be published as a discussion in a future issue of the journal.